

# Novel hybrid silica thin film based on bismuth vanadate and polyoxometalates system: visible-light photochromic behavior and mechanism

ZONG-LAI LIU, GUO-PENG ZHU, ZHENG-YI WANG LI-CHEN ZHAO, BO DONG YONG-HE DONG WEI FENG\*  
*Key Lab of Groundwater Resources and Environment, Ministry of Education, Jilin University, Changchun 130021, P. R. China*

Novel visible-light photochromic silica sol-gel hybrid film was successfully synthesized by blending the composite of bismuth vanadate ( $\text{BiVO}_4$ ) and phosphotungstic acid (PWA). The crystal phase, microstructure, photochromic properties and mechanism were investigated *via X-ray diffraction (XRD)*, transmission electron microscope (TEM), Fourier transform infrared spectroscopy (FT-IR), ultraviolet-visible (UV-Vis) spectra and X-ray photoelectron spectroscopy (XPS). XRD pattern confirmed the existence of  $\text{BiVO}_4$  and PWA in  $\text{SiO}_2$  sol-gel composite films. FT-IR results indicated that the basic structure of  $\text{BiVO}_4$  nanoparticle and the Keggin geometry of PWA were not damaged in the process of compositing and there was a strong interaction between  $\text{BiVO}_4$  and PWA. TEM images showed that PWA with the homogeneous spherical morphology well dispersed in the surface of  $\text{BiVO}_4$  and a part of PWA embedded into  $\text{BiVO}_4$  hybrid film. Irradiated with visible light, the composite film turned to blue from colorless. The hybrid film showed reversible photochromism in the presence of oxygen. According to XPS results, PWA accepted electrons from  $\text{BiVO}_4$  and the photo-reduction process was concerned with photogenerated electron transfer mechanism.

(Received October 12, 2018; accepted June 14, 2019)

*Keywords:* Silica sol-gel, Bismuth vanadate, Polyoxometalates, Hybrid film, Visible-light photochromism

## 1. Introduction

As the unique properties that different wavelengths shining light leads to different colors, photochromic materials have been widely used in information storage, sensor, decorative material, photoelectric conversion device, intelligent switch and national defense [1-3]. Polyoxometalates (POMs) was a kind of promising inorganic photochromic material, which exhibit excellent thermal stability, oxidation stability and mechanical property. Up to now, various POMs-based composite systems have been fabricated by entrapping POMs into inorganic or organic networks [4-7]. However, most of the systems were in response to UV light. But the light source of the ultraviolet lasers exhibited expensive price, which limited its large-scale practical application.

In order to improve the utilization of solar energy, POMs-based composite materials which were in response to visible light have been built. In recent years, a lot of researches on the photochromic properties of heteropolyacid/organic polymer composite films were investigated.

Keggin and Dawson type of  $\text{PMo}_{12}$ ,  $\text{PW}_{12}$ ,  $\text{H}_4\text{W}_{10}\text{O}_{32}$ ,  $\text{SiW}_{12}$ ,  $\text{H}_4\text{GeW}_{12}\text{O}_{40}$  and  $\text{H}_3\text{PW}_{11}\text{MoO}_{40}$  could be used as a light reduction component. Organic polymer composite

commonly were made up by embedding heteropoly acid into organic photochromic films then combining with polyacrylamide (PAM), polyvinyl alcohol (PVA) and polyethylene glycol (PEG), polyvinylpyrrolidone (PVP) and poly(ethyleneimine) (PEI), ethyl cellulose (EC) etc. [8-12] Shi reported a novel type of polyoxometalate- $\text{PMo}_{12}/\text{TiO}_2/\text{Ag}$  composite fibers showed high photocatalytic activity under visible light. The introduction of POM species not only improved the light absorption and redox activity of  $\text{TiO}_2$ , but also promoted the photochemical stability of the complex [13].

$\text{BiVO}_4$  was a promising n-type semiconductor with high chemical stability, photo stability and nontoxicity. Due to its narrow band gap of approximately 2.4-2.8 eV,  $\text{BiVO}_4$  was sensitive to visible light [15]. Herein, we reported a new hybrid film fabricated by introducing the composite of  $\text{BiVO}_4$  and PWA into  $\text{SiO}_2$  sol-gel where the  $\text{SiO}_2$  acted as film-forming agent making the system exhibit excellent uniformity and stability. The experimental results demonstrated that the hybrid film exhibited remarkable photochromic properties upon visible light irradiation and showed reversible photochromism in the presence of oxygen.

## 2. Experimental section

### 2.1. Materials

Phosphate acid (PWA), butyl silicate and ammonium vanadate ( $\text{NH}_4\text{VO}_3$ ) were purchased from Sinopharm Chemical Reagent (China). PWA was purified by recrystallizing twice before use. Bismuth nitrate [ $\text{Bi}(\text{NO}_3)_3 \cdot 5\text{H}_2\text{O}$ ] was purchased from Xilong Chemical Co (Shantou, China). All other chemical reagents were of analytical grade and used as received.

### 2.2. Preparation

For the synthesis of  $\text{BiVO}_4$ ,  $\text{Bi}(\text{NO}_3)_3 \cdot 5\text{H}_2\text{O}$  (4.85g) and  $\text{NH}_4\text{VO}_3$  (1.16g) were dissolved respectively in 10 mL nitric acid ( $\text{HNO}_3$ ) and 20 mL NaOH solution under magnetic stirring. Mixed the two solutions and adjusted the pH to an appropriate extent by adding NaOH into the mixture. With ultrasonic treatment for 30 min, the precursor was got. Transferred the precursor into Teflon-lined stainless steels and the hydrothermal process was conducted at  $180^\circ\text{C}$  for 12 h. Cooling to room temperature, the  $\text{BiVO}_4$  was got after drying the precipitate which was separated using centrifugal machine and washed for several times with ethanol and deionized water.

For the synthesis of  $\text{SiO}_2$  sol-gel, 22.5 mL butyl silicate was dissolved in absolute ethyl alcohol under magnetic stirring. Instill the mixed solution of 9.2 mL absolute ethyl alcohol, 1.8 mL distilled water and 5 mL glycerin. Continue stirring for 5 hours before adding the hydrochloric acid. The achromatous and transparent  $\text{SiO}_2$  sol was obtained overnight [16].

Dissolved 0.3 g PWA in 5 ml ethanol, then added 10 mg  $\text{BiVO}_4$  into the solution to get the mixture. Complex solution of  $\text{BiVO}_4/\text{PWA}/\text{SiO}_2$  was received after dropping the mixture into  $\text{SiO}_2$  sol under stirring for 2 h. Then, the complex solution was dripped on various substrates such as KBr plates copper grids, quartz plates and sili-con grids for different tests using a syringe with a capacity of 100  $\mu\text{l}$  and the film samples were preserved with surrounding humidity less than 60%. The thickness of hybrid film was approximately 2.6  $\mu\text{m}$ , which was measured by a FCT-1030 Film Thickness Measurement System (LCD Lab, Changchun Institute of Optics, Fine Mechanics and Physics, Chinese Academy of Science).

### 2.3. Instrumental analysis

The crystal phase and structures of the samples were characterized by a powder X-ray diffraction (XRD) using D/max-2550 PC for Cu  $K\alpha$  ( $\lambda=1.54056\text{\AA}$ ) radiation at 40kV and 200Ma, where the scanning angle ranged from  $20^\circ$  to  $70^\circ$  of  $2\theta$ . FT-IR spectra were determined by the samples deposited on the KBr pellets with a Nicolet

Impact 410 FT-IR spectrometer in the wavenumber range of 2000–400  $\text{cm}^{-1}$ . The TEM measurement was taken on a JEOL JEM-200CX transmission electron microscopy with dropping complex solution onto the copper grids. Absorption curves of the samples were obtained on a JASCO V-550 UV-vis spectrophotometer with 1 nm optical resolution in the range of 350–900 nm. XPS spectra were recorded by an ESCALAB 250 photoelectron spectrometer to acquire the information on chemical binding energy of hybrid film. Photochromic experiments were carried out using a 300W Xe lamp as the light source and the light was passed through a glass filter in order to guarantee that only the wavelengths longer than 422 nm could be conducted on the photoanode. All measurements were carried out at room temperature.

## 3. Result discussion

Wide-angle XRD was used to identify the crystalline phase of the as-synthesized pure  $\text{BiVO}_4$ , pure PWA and  $\text{BiVO}_4/\text{PWA}/\text{SiO}_2$  composite film. As shown in Fig. 1, the  $2\theta$  values at  $28.7^\circ$ ,  $31.0^\circ$ ,  $42.6^\circ$ ,  $47.1^\circ$  and  $53.7^\circ$  matched well with (1 0 1), (1 1 2), (0 0 4), (2 0 3) and (2 1 3) planes of the monoclinic  $\text{BiVO}_4$  (PDF#48-0744), respectively. No impurity peaks were observed, indicating the high purity of the as-prepared samples. The diffraction peak of  $\text{BiVO}_4$  and PWA was present in the pattern for  $\text{BiVO}_4/\text{PWA}/\text{SiO}_2$  composite films, which implied the existence of  $\text{BiVO}_4$  and PWA in  $\text{SiO}_2$  sol-gel composite films.

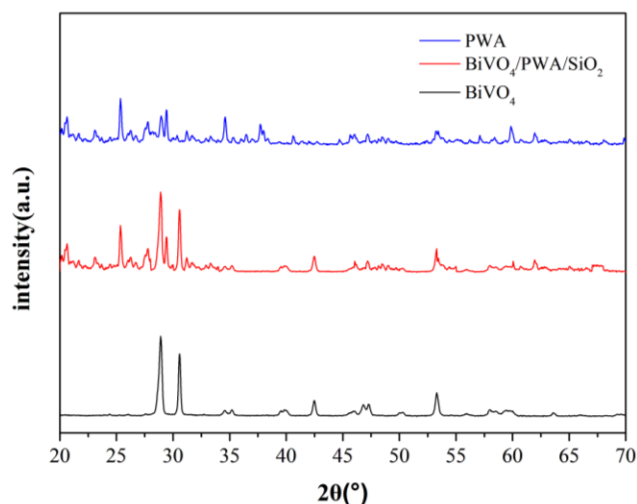


Fig. 1. XRD patterns of different samples

The FT-IR spectrum was inserted in Fig. 2 to confirm the molecular structure and chemical bonds of PWA,  $\text{BiVO}_4$  and  $\text{BiVO}_4/\text{PWA}/\text{SiO}_2$  composite films. In the curve a of pure PWA, the characteristic bands standing for the Keggin geometry at  $1080\text{ cm}^{-1}$ ,  $982\text{ cm}^{-1}$ ,  $890\text{ cm}^{-1}$  and  $802\text{ cm}^{-1}$  belonged to the stretching vibration of P-O<sub>a</sub>, W-O<sub>d</sub>, W-O<sub>b</sub>-W and W-O<sub>c</sub>-W, respectively [17]. In the

composite film (curve c), the P-O<sub>a</sub> vibration had no change in principle. The W-O<sub>b</sub>-W vibration and W-O<sub>c</sub>-W vibration had red shift by 3 cm<sup>-1</sup> and 2 cm<sup>-1</sup>. Both of the results declared that the Keggin geometry was preserved in the composite process and there was a strong interaction between BiVO<sub>4</sub> and PWA [18]. At the same time, the characteristic band at 734 cm<sup>-1</sup> representing BiVO<sub>4</sub> still existed in BiVO<sub>4</sub>/PWA/SiO<sub>2</sub> composite film [19], which indicated that the basic structure of BiVO<sub>4</sub> was not destroyed during the composite process. After visible light irradiation (curve d), the W-O<sub>a</sub> vibration had shift from 1080 cm<sup>-1</sup> to 1082 cm<sup>-1</sup> and W-O<sub>d</sub> vibration had red shift from 980 cm<sup>-1</sup> to 987 cm<sup>-1</sup>, which revealed that the oxidation-reduction reaction indeed happened [8]. The W-O<sub>b</sub>-W vibration had blue shift by 4 cm<sup>-1</sup> and the W-O<sub>c</sub>-W vibration disappeared compared with the unirradiated film. Above all results proved that the reaction of photo-reduction happened and the heteropolyacid accepting electrons transformed into heteropolyblues in the irradiation process [4].

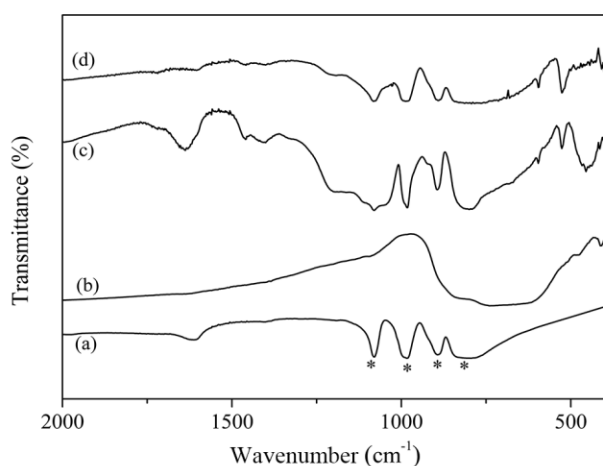


Fig. 2. FT-IR spectra of (a) PWA, (b) BiVO<sub>4</sub>, BiVO<sub>4</sub>/PWA/SiO<sub>2</sub> composite film (c) before and (d) after visible light irradiation

The microstructure of SiO<sub>2</sub> sol-gel film, BiVO<sub>4</sub> and BiVO<sub>4</sub>/PWA/SiO<sub>2</sub> composite film were revealed by TEM images. As shown in Fig. 3a, the SiO<sub>2</sub> sol-gel film was homogeneous with no particle clouds. Spherical BiVO<sub>4</sub> dispersed uniformly in the system with the size of 500 nm (Fig. 3b). From the inset Fig. 3c, the BiVO<sub>4</sub>/PWA/SiO<sub>2</sub> composite had regular diameter similar to BiVO<sub>4</sub> which indicated that the PWA had a small size and PWA wrapped around BiVO<sub>4</sub>. The HRTEM (Fig. 3d) showed that PWA nanoparticles attached to the surface of BiVO<sub>4</sub> and a part of PWA embedded into BiVO<sub>4</sub>. This consequence indicated there was a strong interaction between BiVO<sub>4</sub> and PWA during the composite process, which was consistent with the FT-IR results.

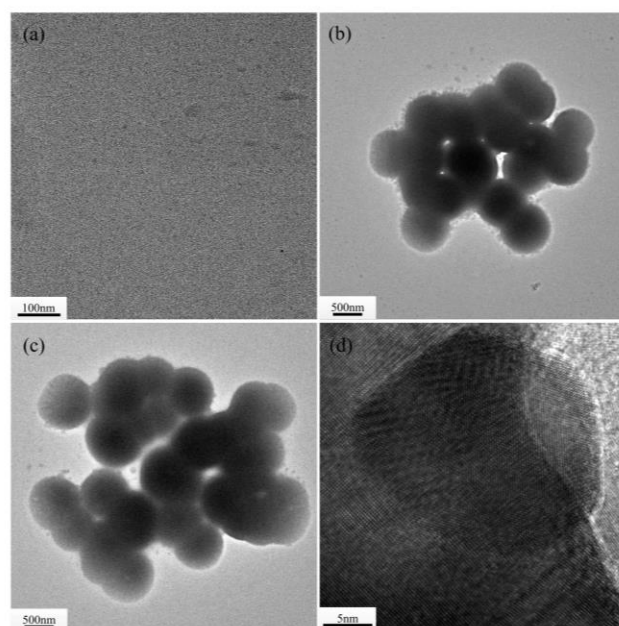


Fig. 3. TEM images of (a) BiVO<sub>4</sub> and (b-d) BiVO<sub>4</sub>/PWA/SiO<sub>2</sub> composite film before visible light irradiation

UV-vis absorption spectrum of the composite film before and after irradiation was illustrated in Fig. 4. Before visible light irradiation, there were no significant absorptions of the composite film at 350 nm-900 nm. Along with the visible light irradiation, the composite film turned to blue from colorless, and two new broad absorption peaks appeared at 490 nm and 750 nm, which were due to the intensity-enhanced d-d transition and metal-to-metal extra intervalence charge transfer (IVCT) (W<sup>5+</sup>→W<sup>6+</sup>), respectively [14]. The generating of heteropolyblue indicated the phenomenon of electron transfer happened between BiVO<sub>4</sub> and PWA [20], which was in accord with FT-IR results.

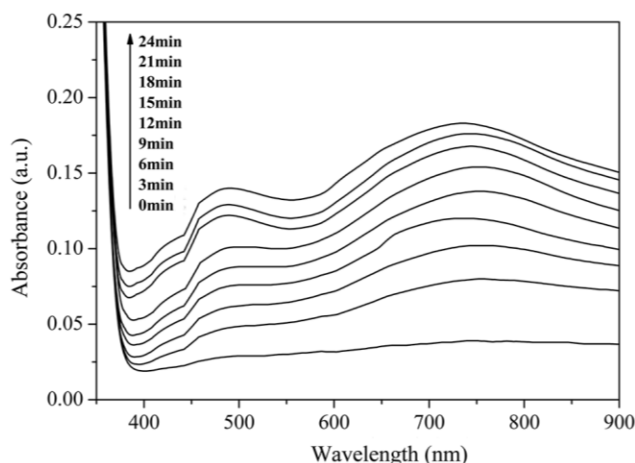


Fig. 4. UV-vis absorption spectrum of the composite film before and after irradiation

The kinetics of the coloration process was investigated by monitoring the absorbance changes at 750 nm as a function of irradiation time (Fig. 5) and the experimental data were treated with the following integrated equation [21]:

$$-\ln(A_{\infty}-A_t)=kt+b$$

The  $k$  was rate constant.  $A_{\infty}$  and  $A_t$  were the observed reflection data measured at the end and at the time of the reaction, respectively. The photochromic process of the PWA/SiO<sub>2</sub> and BiVO<sub>4</sub>/PWA/SiO<sub>2</sub> hybrid film followed first-order kinetic with rate constants  $k_1=0.189 \text{ min}^{-1}$  and  $k_2=0.214 \text{ min}^{-1}$  respectively. This confirmed that introduction of BiVO<sub>4</sub> can improve the performance of photochromic.

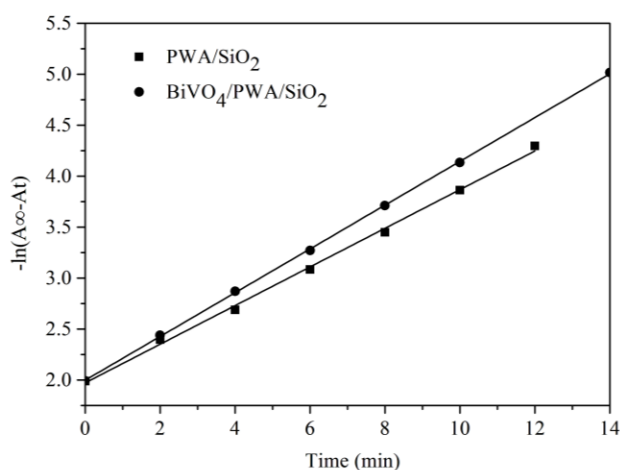


Fig. 5. The kinetic plot of the photochromic process for PWA/SiO<sub>2</sub> and BiVO<sub>4</sub>/PWA/SiO<sub>2</sub> composite film

The bleaching process of the composite film sheltered from light at room temperature was described in Fig. 6. The absorbance became 60% of the original without visible light for 6 h at room temperature. In particular, the colored film heated at 60 °C bleached completely in 10 min, which proved that the heat influenced bleaching speed of the composite film. The colored film stayed to be blue without exposed to oxygen, such as protected by nitrogen or kept in vacuum, revealing that the oxygen which could oxidize W(V) to W(VI) was an important factor for the bleaching process [4].

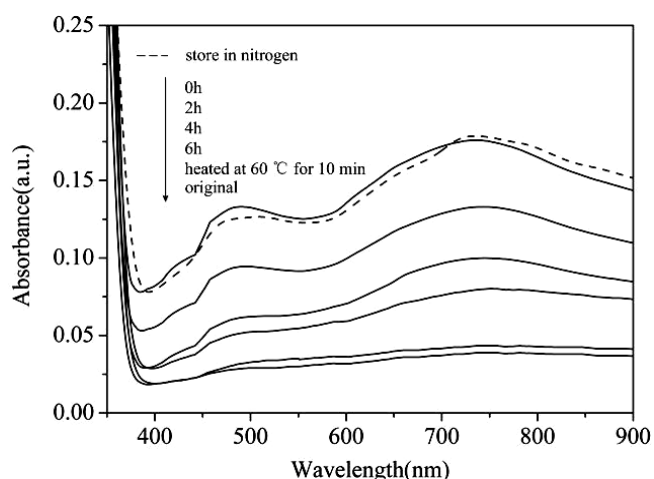


Fig. 6. The bleaching process of BiVO<sub>4</sub>/PWA/SiO<sub>2</sub> composite film after irradiation

The coloration-decoloration process was displayed in Fig. 7. As shown, the coloration-decoloration cycle could repeat many times. During the 7 cycles in Fig. 7, the maximum of absorbance ranged from 0.180 to 0.230, which proved that the BiVO<sub>4</sub>/PWA/SiO<sub>2</sub> composite film had excellent photochromic performance, including high-photochromic response, high-stability and good reversibility [22]. With the increase of irradiation times, the reversible growth of the composite film was increased. From the infrared spectrum analysis results, the interaction between PWA and BiVO<sub>4</sub> increases with the increase of coloration-decoloration process. The enhancement of the interaction led to the enhancement of photochromic efficiency, resulting in a better reversibility of the composite film.

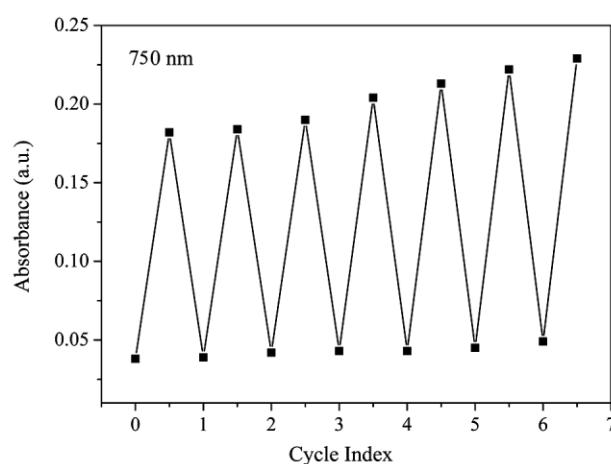


Fig. 7. The coloration-decoloration process of BiVO<sub>4</sub>/PWA/SiO<sub>2</sub> composite film

XPS spectra, which were effective to explore the electronic structure changes and photochromic mechanism of composite film, were illustrated in Fig. 8a and b. W<sub>4f</sub>

binding energies could be separated into two degenerated energy levels,  $W_{4f_{7/2}}$  and  $W_{4f_{5/2}}$  by employing Gaussian deconvolution and the energy values were listed in Table 1 [23]. For the composite film before visible light irradiation, there was no peak of  $W^{5+}$  and the binding energy values of  $W^{6+}$  were 34.82 and 37.79 eV. After visible light irradiation, the  $W_{4f}$  doublet of  $W^{5+}$  and  $W^{6+}$  were all detected. The binding energy values of  $W^{5+}$  were 33.70 and 36.57 eV and those of  $W^{6+}$  were 34.98 and 37.73 eV. Obviously, the width of characteristic bands for  $W^{6+}$  was smaller after irradiation. All of the phenomenons above demonstrated the chemical microenvironment of W changed during the process of photo-production [24]. Besides, the chemical valences degenerate peak areas of the XPS spectra were calculated by integral operation to estimate the photo-reductive extent of the composite film. The appearance of  $W^{5+}$  characteristic signal (the ratio was

0.59) involved the photo-reduction took place in the process of visible light irradiation.

Table 1. Binding energies of  $W_{4f}$  energy level and  $W^{5+}/W^{6+}$  ratios of  $BiVO_4/PWA/SiO_2$  composite film after irradiation

Sample	$W^{5+}$		$W^{6+}$		$W^{5+}/W^{6+}$ Ratios
	$4f_{5/2}$	$4f_{7/2}$	$4f_{5/2}$	$4f_{7/2}$	
Before	-	-	34.82	37.79	-
After	33.70	36.57	34.98	37.73	0.59

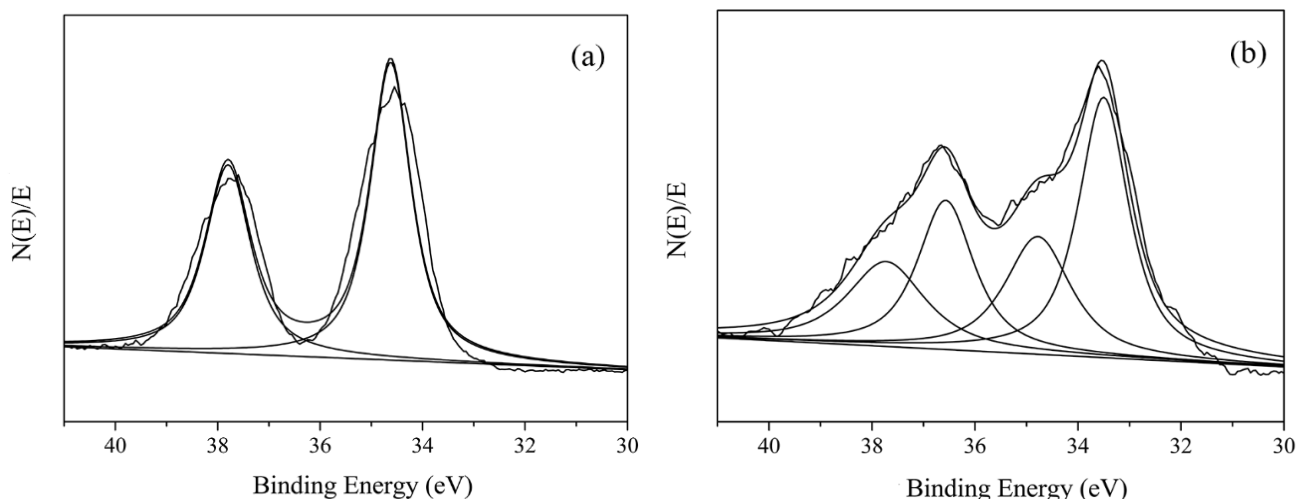


Fig. 8. XPS spectra of  $W_{4f}$  energy level of the  $BiVO_4/PWA/SiO_2$  hybrid film (a) without visible light irradiation, (b) visible light irradiation

The photochromic mechanism of composite film was further investigated according to the energy levels of  $BiVO_4$  and PWA and the sketch was illustrated in Fig. 9. Motivated by visible light,  $BiVO_4$  could produce plenty of electrons. As for the PWA conduction band (CB) had lower energy, the electrons produced by  $BiVO_4$  excited from  $BiVO_4$  conduction band to PWA conduction band and combined with the PWA absorbed on the surface of  $BiVO_4$ . With the occurring of photo-reduction, PWA accepted the electrons and generated heteropolyblues. So, it could be conclude that the photochromic process of  $BiVO_4/PWA/SiO_2$  composite film was conducted by the electron transfer mechanism.

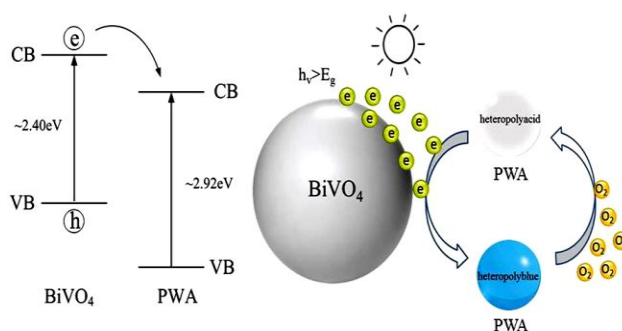


Fig. 9. Schematic presenting the electron transfer between PWA and  $BiVO_4$  for  $BiVO_4/PWA/SiO_2$  composite film

#### 4. Conclusion

Novel photochromic hybrid film with SiO<sub>2</sub> sol-gel was prepared by blending the composite of BiVO<sub>4</sub> and PWA. The film turned to blue from colorless with the irradiation of visible light, and showed reversible photochromic properties in the presence of oxygen. The coloration-decoloration circle could repeat dozens of times and the photo-reduction process occurred according to electron transfer mechanism. By combined the light-sensitive material BiVO<sub>4</sub> with polyoxometalate, this study settled the theoretical foundation for reversibility and fatigue resistance research of photochromic materials.

#### Acknowledgment

The author was grateful to the National Natural Science Foundation of China (No. 61774073), Open Project of State Key Laboratory of Inorganic Synthesis and Preparative Chemistry, Jilin University (No. 2016-25) and Science and Technology Development Program of Jilin province (No. 20170101086JC).

#### References

- [1] K. Börjesson, M. Herder, L. Grubert, D. Duong, A. Salleo, S. Hecht et al., *Journal of Materials Chemistry C* **3**, 4156 (2015).
- [2] Q. Meng, L. Fang, T. Han, S. Huang, S. Xie, *Sensors and Actuators B: Chemical* **228**, 144 (2016).
- [3] T. Benelli, L. Mazzocchetti, G. Mazzotti, F. Paris, E. Salatelli, L. Giorgini, *Dyes and Pigments* **126**, 8 (2016).
- [4] J. Chen, Y. Liu, D.-Q. Xiong, W. Feng, W.-M. Cai, *Thin Solid Films* **516**, 2864 (2008).
- [5] M. Jiang, E. Wang, G. Wei, L. Xu, Z. Li, *Journal of Colloid and Interface Science* **275**, 596 (2004).
- [6] B. Qin, H. Chen, H. Liang, L. Fu, X. Liu, X. Qiu et al., *Journal of the American Chemical Society* **132**, 2886 (2010).
- [7] H. El Moll, A. Dolbecq, Il. M. Mbomekalle, Jr. M. Marrot, P. Deniard, Rm. Dessapt et al., *Inorganic Chemistry* **51**, 2291 (2012).
- [8] M. Jiang, E. B. Wang, G. Wei et al., *New Journal of Chemistry* **27**(9), 1291 (2003).
- [9] Diana M. Fernandes, C. Freire et al., *Journal of Applied Electrochemistry* **44**(5), 655 (2014).
- [10] H. F. Bao, Y. W. Xiang, W. Feng et al., *Colloid and Polymer Science* **292**(11), 2883 (2014).
- [11] X. F. Jing, D. L. Zou, W. Feng et al., *Inorganic Chemistry Communications* **46**, 149 (2014).
- [12] X. J. Peng, Y. Zhang, W. Feng et al., *Journal of Molecular Structure* **1041**, 139 (2013).
- [13] H. Shi, Y. Yu, Y. Zhang et al., *Applied Catalysis B Environmental* **280** (2018).
- [14] K. Kumamoto, K. Tsuchibashi, A. D. Pramata et al., *Journal of Physical Chemistry C* **121**, 13515 (2017).
- [15] O. F. Lopes, K. T. Carvalho, A. E. Nogueira, W. Avansi, C. Ribeiro, *Applied Catalysis B: Environmental* **188**, 87 (2016).
- [16] X. Wang, Y. Sun, C. Liu, W. Feng, D. Zou, *RSC Advances* **5**, 49153-8 (2015).
- [17] X.-J. Peng, Y. Zhang, W. Feng, L.-M. Ai, J. Chen, F.-J. Zhang, *Journal of Molecular Structure* **1041**, 139 (2013).
- [18] J. Chen, S.-L. Liu, W. Feng, X.-J. Bao, F.-L. Yang, *Optical Materials* **35**, 973 (2013).
- [19] W. Liu, G. Zhao, L. Chang, *Applied Surface Science* **357**, 1053 (2015).
- [20] H. Qi, Y. Liu, W. Feng, Y. Zhu, *Science in China Series B: Chemistry* **52**, 169 (2009).
- [21] X.-Y. Wang, Q. Dong, Q.-L. Meng, J.-Y. Yang, W. Feng, X.-K. Han, *Applied Surface Science* **316**, 637 (2014).
- [22] Y. Sun, X. Wang, Y. Lu, L. Xuan, S. Xia, W. Feng et al., *Chemical Research in Chinese Universities* **30**, 703 (2014).
- [23] Y. Chen, G. Yu, F. Li, C. Xie, G. Tian, *Journal of Materials Chemistry C* **1**, 3842 (2013).
- [24] X. Jing, Q. Meng, D. Zou, W. Feng, X. Han, *Materials Letters* **136**, 229 (2014).

\*Corresponding author: weifeng@jlu.edu.cn